A Two-Dimensional Potential Energy Surface and Associated Quantum States for the Ring-Puckering Vibrations of Two Equivalent Rings: A Study of Bicyclo[3.3.0]oct-1,5-ene

3 AUTHORS:

Daniel Autrey
Fayetteville State University
17 PUBLICATIONS   206 CITATIONS

SEE PROFILE

Niklas Meinander
National Defense University, Finland
48 PUBLICATIONS   577 CITATIONS

SEE PROFILE

Jaan Laane
Texas A&M University
265 PUBLICATIONS   4,252 CITATIONS

SEE PROFILE

A Two-Dimensional Potential Energy Surface and Associated Quantum States for the Ring-Puckering Vibrations of Two Equivalent Rings: A Study of Bicyclo[3.3.0]oct-1,5-ene

Daniel Autrey, Niklas Meinander,[†] and Jaan Laane*

Department of Chemistry, Texas A&M University, College Station, Texas 77843-3255

Received: July 30, 2003; In Final Form: October 14, 2003

The results of ab initio calculations have been utilized to produce plausible two-dimensional energy surfaces of the form $V = a(x_1^4 + x_2^4) + b(x_1^2 + x_2^2) + cx_1^2x_2^2 + dx_1x_2$ for the ring-puckering vibrations of bicyclo-[3.3.0]oct-1,5-ene, with each coordinate representing the puckering motion of one ring. Polynomial expressions for the kinetic energy (reciprocal reduced mass) associated with the puckering motions of the rings were developed and utilized. These expressions were used together with the potential energy surfaces to calculate the quantum states and spectroscopic transitions for the puckering motions. The effect of varying the potential energy parameters c (ring-to-ring interaction) and d (cis-trans energy difference) on the energy levels and transitions was examined. The expected spectra are very rich and complex.

Introduction

In the preceding paper[1] we presented the vibrational spectra and ab initio calculations for bicyclo[3.3.0]oct-1,5-ene (BCO). The analysis of the infrared and Raman spectra together with the ab initio results demonstrated that the two five-member rings of this molecule are puckered in either the cis or trans configurations. The ab initio calculations also predicted relative energies for the C_{2v}, C_{2h}, D_{2h}, and C_s structures of this molecule. In the present paper we derive two-dimensional potential energy surfaces for the ring-puckering using the ab initio computed potential energies of the different structures and use these surfaces to characterize the puckering quantum states and the vibrational spectrum of the large amplitude puckering motion.

The ring-puckering far-infrared spectrum of BCO is expected to be weak as the out-of-plane ring-bending motions generate only a small dipole moment change. Moreover, the compound boils at 141°C and thus the sample must be heated substantially to obtain sufficient vapor pressure for recording the gas phase spectrum. This is not a trivial task for far-infrared spectra since the window materials either do not withstand high temperatures (polyethylene) or transmit poorly (silicon). In addition, upon heating the long-path cell, water adsorbed on the cell surfaces vaporizes and causes cluttering of the far-infrared spectrum with numerous strong water bands. Consequently, we have only been able to obtain some poor quality far-infrared (FIR) spectra of BCO showing a broad unresolved absorption maximum around 200 cm^{-1} and a few resolved bands not attributed to water, which can only support our theoretical findings in a general way.

The nature of the potential energy surface, the puckering quantum states, and the spectral features derived in this work should be similar to those of other molecules with similar structure. The present results should thus provide a reasonable starting point for the analysis of far-IR spectra recorded for such molecules.
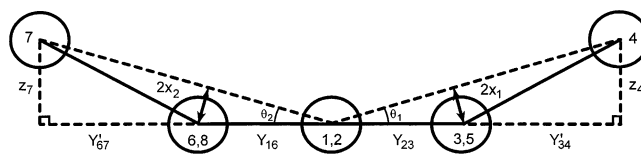

Figure 1. Definition of the ring-puckering coordinates x_1 and x_2.

The Vibrational Hamiltonian

In a number of previous studies of large amplitude ring motions we have carried out two-dimensional calculations for molecules where the two vibrations considered are different.[2-5] For example, for phthalan[6-8] or 1,3-benzo-dioxole,[9,10] the ring-puckering and ring-flapping modes were considered. In the present case for BCO, the two puckering vibrations are equivalent. Hence, the vibrational Hamiltonian[2-6,11]

$$H = -\frac{\hbar^2}{2}\left[\frac{\partial}{\partial x_1}g_{44}(x_1,x_2)\frac{\partial}{\partial x_1} + \frac{\partial}{\partial x_2}g_{55}(x_1,x_2)\frac{\partial}{\partial x_2} + \frac{\partial}{\partial x_1}g_{45}(x_1,x_2)\frac{\partial}{\partial x_2} + \frac{\partial}{\partial x_2}g_{45}(x_1,x_2)\frac{\partial}{\partial x_1}\right] + V(x_1,x_2) \quad (1)$$

is symmetric with respect to permutation of the puckering coordinates of the two rings. The coordinates x_1 and x_2 are defined in Figure 1. The kinetic energy (reciprocal reduced mass) expressions, g_{44}, g_{55}, and g_{45}, are explained below, and V is the potential energy, for which the simplest representation in the present case is

$$V = a(x_1^4 + x_2^4) + b(x_1^2 + x_2^2) + cx_1^2x_2^2 + dx_1x_2 \quad (2)$$

The coefficient a mostly reflects angle strain of the rings, while b, which is negative, determines the barriers to planarity of the rings, which arise from $-CH_2-CH_2-$ torsional interactions. The third term models the ring-to-ring interaction and the last the asymmetry, which causes the puckering of the two rings in the same or opposite directions to result in different energies. Other

* Corresponding author.
† Permanent Address: Department of Technology, National Defence College, Helsinki, Finland.

410 *J. Phys. Chem. A, Vol. 108, No. 3, 2004*

Autrey et al.

TABLE 1: Components of the Bond Vectors $\vec{u}_i = a_i \vec{i} + b_i \vec{j} + c_i \vec{k}$ for the In-Phase and Out-of-Phase Ring-Bending Vibrations of Bicyclo[3.3.0]-oct-1(5)-ene (BCO)[a]

	a_i	b_i	c_i
$\vec{u_1}$	R_1	0	0
$\vec{u_2}$	X_{23}	Y_{23}	0
$\vec{u_3}$	$-X_{34}$	Y_{34}'	z_4
$\vec{u_4}$	$-X_{34}$	$-Y_{34}'$	$-z_4$
$\vec{u_5}$	X_{23}	$-Y_{23}$	0
$\vec{u_6}$	$-X_{16}$	$-Y_{16}$	0
$\vec{u_7}$	X_{67}	$-Y_{67}'$	z_7
$\vec{u_8}$	X_{67}	Y_{67}'	$-z_7$
$\vec{u_9}$	$-X_{16}$	Y_{16}	0
$\vec{u_{10}}$	$p_{3x} + v_{3x}$	$p_{3y} + v_{3y}$	$p_{3z} + v_{3z}$
$\vec{u_{11}}$	$p_{3x} - v_{3x}$	$p_{3y} - v_{3y}$	$p_{3z} - v_{3z}$
$\vec{u_{12}}$	0	$p_{4y} + v_{4y}$	$p_{4z} + v_{4z}$
$\vec{u_{13}}$	0	$p_{4y} - v_{4y}$	$p_{4z} - v_{4z}$
$\vec{u_{14}}$	$-(p_{3x} + v_{3x})$	$-(p_{3y} + v_{3y})$	$-(p_{3z} + v_{3z})$
$\vec{u_{15}}$	$-(p_{3x} - v_{3x})$	$-(p_{3y} - v_{3y})$	$-(p_{3z} - v_{3z})$
$\vec{u_{16}}$	$-(p_{8x} + v_{8x})$	$-(p_{8y} + v_{8y})$	$-(p_{8z} + v_{8z})$
$\vec{u_{17}}$	$-(p_{8x} - v_{8x})$	$-(p_{8y} - v_{8y})$	$-(p_{8z} - v_{8z})$
$\vec{u_{18}}$	0	$p_{7y} + v_{7y}$	$p_{7z} + v_{7z}$
$\vec{u_{19}}$	0	$p_{7y} - v_{7y}$	$p_{7z} - v_{7z}$
$\vec{u_{20}}$	$p_{8x} + v_{8x}$	$p_{8y} + v_{8y}$	$p_{8z} + v_{8z}$
$\vec{u_{21}}$	$p_{8x} - v_{8x}$	$p_{8y} - v_{8y}$	$p_{8z} - v_{8z}$

a

$$z_4 = \frac{2x_1}{Y_{23}}\left[\sqrt{Y_{23}^2 - 4x_1^2} + \sqrt{Y_{34}^2 - 4x_1^2}\right]; z_7 =$$

$$\frac{2x_2}{Y_{16}}\left[\sqrt{Y_{16}^2 - 4x_2^2} + \sqrt{Y_{67}^2 - 4x_2^2}\right]$$

$$X_{23} = X_{16} = R_2 \sin\left(\gamma - \frac{\pi}{2}\right); Y_{23} = Y_{16} = R_2 \cos\left(\gamma - \frac{\pi}{2}\right)$$

$$X_{34} = X_{23} + \frac{R_1}{2}; Y_{34} = \sqrt{R_3^2 - X_{34}^2}; Y_{34}' = \sqrt{Y_{34}^2 - z_4^2}$$

$$X_{67} = X_{16} + \frac{R_1}{2}; Y_{67} = \sqrt{R_3^2 - X_{67}^2}; Y_{67}' = \sqrt{Y_{67}^2 - z_7^2}$$

$$\vec{p_3} = \vec{p}(R_4,T_2,\vec{u_2},\vec{u_3}) = R_4 \cos\left(\frac{T_2}{2}\right)\frac{\left[\frac{\vec{u_2}}{R_2} \cdot \frac{\vec{u_3}}{R_3}\right]}{\left|\frac{\vec{u_2}}{R_2} - \frac{\vec{u_2}}{R_3}\right|} = R_4\cos\left(\frac{T_2}{2}\right)\frac{\left[\frac{\vec{u_2}}{R_2} - \frac{\vec{u_3}}{R_3}\right]}{2\cos\left(\frac{\beta_1}{2}\right)}$$

$$\vec{v_3} = \vec{v}(R_4,T_2,\vec{u_2},\vec{u_3}) = R_4 \sin\left(\frac{T_2}{2}\right)\frac{\vec{u_2} \times \vec{u_3}}{|\vec{u_2} \times \vec{u_3}|} = R_4 \sin\left(\frac{T_2}{2}\right)\frac{\vec{u_2} \times \vec{u_3}}{R_2R_3 \sin\beta_1}$$

$$\vec{p_4} = \vec{p}(R_5,T_3,\vec{u_3},\vec{u_4}); \vec{v_4} = \vec{v}(R_5,T_3,\vec{u_3},\vec{u_4})$$

$$\vec{p_7} = \vec{p}(R_5,T_3,\vec{u_7},\vec{u_8}); \vec{v_7} = \vec{v}(R_5,T_3,\vec{u_7},\vec{u_8})$$

$$\vec{p_8} = \vec{p}(R_4,T_2,\vec{u_8},\vec{u_9}); \vec{v_8} = \vec{v}(R_4,T_2,\vec{u_8},\vec{u_9})$$

Constants: $R_1 = 1.336$; $R_2 = 1.496$; $R_3 = 1.558$; $R_4 = 1.092$;

$$R_5 = 1.088$$

$$\gamma = 113.2°; T_2 = 106.6°; T_3 = 106.9°$$

possible terms in a two-dimensional potential function modeling the interaction between the rings, such as $x_1^3x_2$ and $x_1x_2^3$, were deemed to be unnecessary in this analysis.

The Kinetic Energy Part of the Hamiltonian

We have previously described the utilization of vector methods for determining the kinetic energy expressions for a variety of molecules examined either one- or two-dimensionally.[12–17] What are required are the expressions showing how the coordinates of each atom change in the center of mass system of the molecule as functions of the vibrational coordinates, in this case the puckering coordinates, x_1 and x_2, which
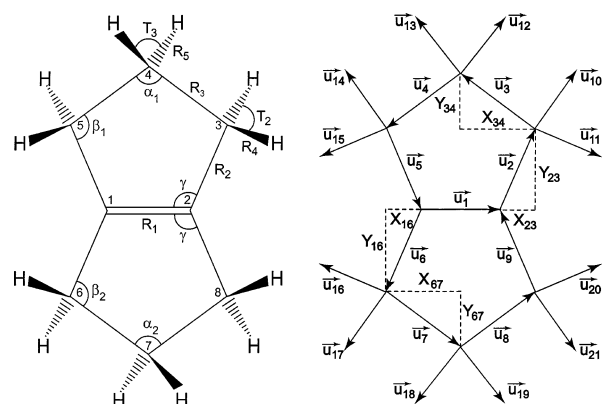
Figure 2. Coordinate vectors for defining the atom positions of BCO as a function of x_1 and x_2.

are defined in Figure 1. This allows calculation of the derivatives of the type $\partial \mathbf{r}_i/\partial x_j$, where the $\mathbf{r}_i$ are the coordinate vectors of the different atoms i and $j = 1$ or 2. These are used to set up the 5×5 $\mathbf{G}^{-1}$ matrix which can be inverted to obtain the $g_{44} = g_{55}$ and g_{45} elements as functions of x_1 and x_2. Finally, polynomial expressions in the two coordinates are fitted to the surfaces thus determined.

Figure 2 shows the definition of the vectors used to define the atom positions, and Table 1 presents the expressions for the components of each vector ($\vec{u}_i = a_i\vec{i} + b_i\vec{j} + c_i\vec{k}$) as functions of the puckering coordinates. As the ab initio results shown in the preceding paper[1] indicate, the true puckering motion involves small changes in all bond lengths and angles. We use a slightly simplified model for the motion here, however, keeping all bond lengths and angles fixed and only allowing the angle β to vary as the apex atoms move in a plane perpendicular to the plane defined by the rest of the skeletal carbon atoms. The position vectors of the hydrogen atoms of the CH$_2$ groups are defined in terms of their components in the direction of the bisector of the CCC angle, α or β, formed by the two adjacent skeletal carbon atoms and the carbon atom of the CH$_2$ group, the $\vec{p}$ vectors, and in the direction perpendicular to the CCC plane, the $\vec{v}$ vectors. We do not consider flapping between the two ring systems in this work, so the apex carbon atoms are the only skeletal atoms allowed to move. Using our usual procedures[12–17] and the calculated ab initio D_{2h} structure shown in Figure 2 of the preceding paper,[1] we obtain the following kinetic energy expressions for the structure with all skeletal carbons except the ones performing the puckering motions being coplanar:

$$g_{44}(x_1,x_2) = 0.00695594 - 0.02936782x_1^2 -$$
$$0.08068994x_1^4 + 0.77221505x_1^6 + 0.0000018x_2^2 -$$
$$0.00571168x_2^4 + 0.0335976x_2^6 + 0.00841432x_1^2x_2^2 -$$
$$0.00998679x_1^3x_2 - 0.00879112x_1x_2^3 + 0.00189241x_1x_2$$
$$(3)$$

$$g_{55}(x_1,x_2) = 0.00695594 + 0.0000018x_1^2 -$$
$$0.00571168x_1^4 + 0.0335976x_1^6 - 0.02936824x_2^2 -$$
$$0.08068994x_2^4 + 0.77221505x_2^6 + 0.00841432x_1^2x_2^2 -$$
$$0.00879112x_1^3x_2 - 0.00998679x_1x_2^3 + 0.00189241x_1x_2$$
$$(4)$$

and

$$g_{45}(x_1,x_2) = -0.00163297 + 0.00522358x_1{}^2 +$$
$$0.02660472x_1{}^4 - 0.20828241x_1{}^6 + 0.00522358x_2{}^2 +$$
$$0.02660472x_2{}^4 - 0.20828241x_2{}^6 - 0.01290496x_1{}^2x_2{}^2 +$$
$$0.03336610x_1{}^3x_2 + 0.03336610x_1x_2{}^3 - 0.00966326x_1x_2$$
$$(5)$$

The corresponding surfaces are shown in Figure 3. As expected, g_{44} and g_{55} show considerable coordinate dependence on x_1 and x_2, respectively, but only a little on the other coordinate. The cross kinetic energy term g_{45} depends equally on both coordinates (as it must) as well as on whether the x_1 and x_2 have the same or opposite signs. Thus the degeneracy of the lowest puckering states of the *cis*- and *trans*-conformations of the molecule is lifted already by the kinetic energy contribution to the Hamiltonian. The same expressions, eqs 3−5, were also used in the calculation of the vibrational energies for the potential energy model derived for the slightly flapped molecule, as described below. It should be noted that the leading terms for g_{44}, g_{55}, and g_{45} are by far the most important for the calculation of the quantum states, and these are obtained from the structure calculated for the planar form. Thus, while the vibrational description characterized by Table 1 may be somewhat imperfect and may differ a bit from the ab initio pathway, this will affect the calculation of the quantum states only slightly.

The Potential Energy Part of the Hamiltonian

Unlike in most of our previous work, where the potential energy surfaces (PES) have been derived empirically from the observed transitions, here it is calculated from the relative energies of the energy minima of the C_{2v}, C_{2h}, D_{2h}, and C_s ab initio structures, as described in the preceding paper.[1] Table 2 summarizes the relative conformational energies calculated for four different structures using two different basis sets. Results for both the flapped and planar conformations are shown. The MP2/cc-pvtz triple-ζ calculations should provide the best results.

The ab initio calculations predict a small flapping angle between the two rings at the potential energy minimum, which occurs 164 cm^{-1} (triple-ζ value) below the energy of the cis (C_{2v}) form. However, we have studied the planar model shown in Figure 1 for which all but the apex carbon atoms remain in the plane (nonflapped model) as well as the flapped molecule. The potential energy parameters for the function in eq 2 for the planar molecule were determined to be

$$a = 1.163 \times 10^6 \text{ cm}^{-1}/\text{Å}^4$$
$$b = -2.955 \times 10^4 \text{ cm}^{-1}/\text{Å}^2$$
$$d = -2.571 \times 10^3 \text{ cm}^{-1}/\text{Å}^2 \qquad (6)$$

and c was taken to be zero. Table 3 compares the energy values for this potential energy surface to those from the ab initio calculations. The table also compares the coordinate values for the energy minima. It can be seen that the parameters in eq 6 above reproduce the energies and the minima very well. Moreover, the values correspond well to those determined for cyclopentene.[17] The puckering motion of a single ring has a barrier to planarity of 220 cm^{-1} for BCO, according to the ab initio calculations, whereas cyclopentene has a barrier of 232 cm^{-1}. The cyclopentene dihedral angle[18] is 26° compared to 24° for the cis structure (26° for the W-shaped structure) of this model. The potential energy surface for the parameters in eq 6 is shown in Figure 4.
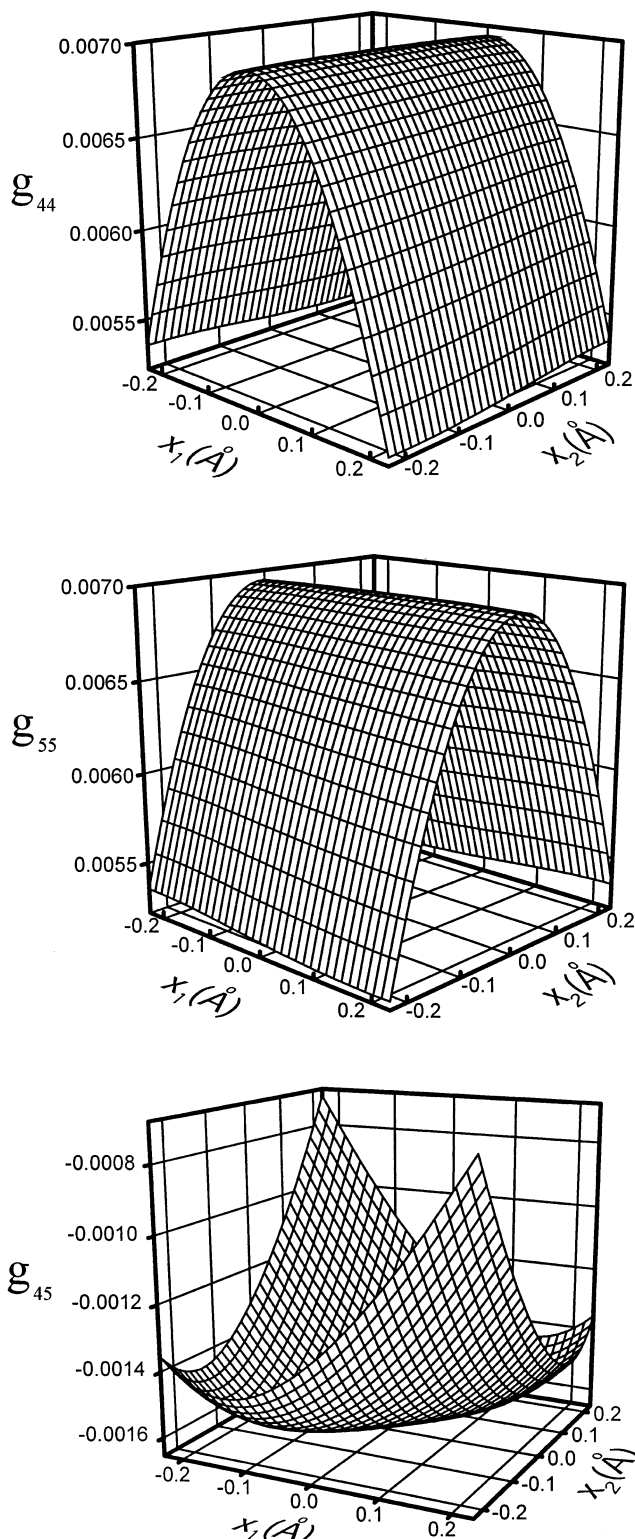

Figure 3. Kinetic energy functions for BCO.

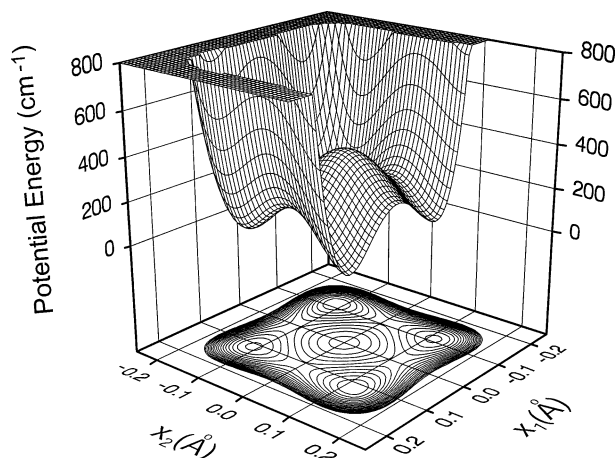**TABLE 2: Calculated Conformational Energies (cm^{-1}) for BCO Structures**

basis set	model	cis	trans	C_s	planar
MP2/cc-pvtz	with flapping	0	229	348	572
MP2/cc-pvtz	no flapping	0	65	220	408
MP2/6-31+G*	with flapping	0	228	380	633
MP2/6-31+G*	no flapping	0	84	267	490

We have also calculated the potential energy surface and quantum states for the flapped molecule, which has an equilibrium structure in which each ring is bent out of the plane by

TABLE 3: Comparison of Potential Energy Surfaces for BCO

parameter	function I (no-flapping)[a]		function II (with flapping)[b]	
	ab initio	eqs 2 and 6	ab initio	eqs 2 and 7
$E_{planar} - E_{cis}$	408.0 cm^{-1}	408.8 cm^{-1}	571.6 cm^{-1}	571.5 cm^{-1}
$E_{trans} - E_{cis}$	65.3 cm^{-1}	65.3 cm^{-1}	229.0 cm^{-1}	229.0 cm^{-1}
$E_{saddle} - E_{cis}$	220.2^{c}cm^{-1}	220.3^{c}cm^{-1}	348.0^{c}cm^{-1}	346.6^{c}cm^{-1}
x^{min}(cis)	0.115 Å	0.115 Å	0.125 Å	0.125 Å
x^{min}(trans)	0.109 Å	0.110 Å	0.109 Å	0.110 Å
dihedral angle (cis)	24.0°	24.0°	26.1°	26.1°
dihedral angle (trans)	22.6°	23.0°	22.6°	23.0°

^{a} $V = 1.163 \times 10^6 (x_1^4 + x_2^4) - 2.955 \times 10^4 (x_1^2 + x_2^2) - 2.571 \times 10^3 x_1 x_2$ ^{b} $V = 1.170 \times 10^6 (x_1^4 + x_2^4) - 3.244 \times 10^4 (x_1^2 + x_2^2) - 8.259 \times 10^3 x_1 x_2$ ^{c} Calculated to be on the x_1 and x_2 axis; the actual saddle point energy is slightly higher (0.8 and 13.4 cm^{-1} for functions I and II, respectively).

Figure 4. Potential energy surface for BCO calculated from ab initio conformational energies (nonflapped model).

3.7° (172.6° flapping angle). The potential energy parameters obtained for this structure are

$$a = 1.170 \times 10^6 \text{ cm}^{-1}/\text{Å}^4$$
$$b = -3.244 \times 10^4 \text{ cm}^{-1}/\text{Å}^2$$
$$d = -8.259 \times 10^3 \text{ cm}^{-1}/\text{Å}^2 \qquad (7)$$

Table 3 also shows the agreement between this PES and the ab initio calculation (triple-ζ). For this PES the cis well is considerably deeper and there is a much greater energy difference (229 cm^{-1}) between the cis and trans wells. The potential energy surface for the parameters in eq 7 is shown in Figure 5.

Calculations of Quantum States and Vibrational Transition Intensities

We have calculated the quantum states and the vibrational transitions for the potential surfaces with the parameters of eqs 6 and 7 using the computer programs we have described elsewhere.[2-5,11] The prediagonalized one-dimensional basis functions were calculated using 100 harmonic basis functions ($\nu = 200$ cm^{-1}). The two-dimensional problem was solved in a (20 × 20) basis using the 20 lowest energy prediagonalized one-dimensional basis functions for each coordinate. The density of vibrational states for these potential surfaces is quite high, being of the order of one level for every 10 cm^{-1} on average. The number of levels between the ground state and 1000 cm^{-1}
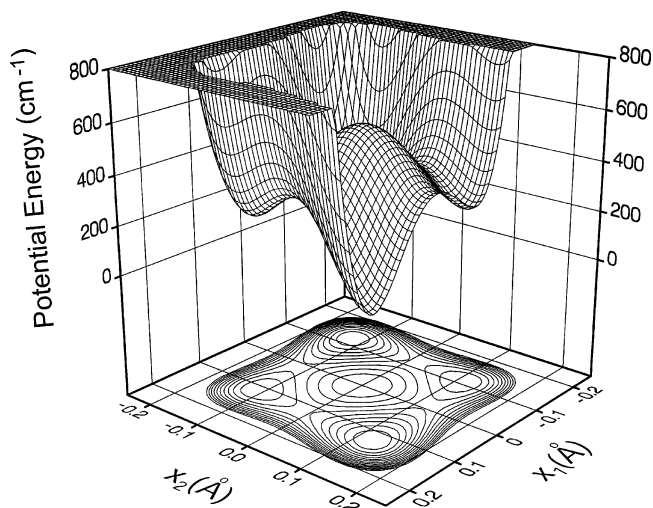
Figure 5. Potential energy surface for BCO calculated from ab initio conformational energies (flapped model).

above that is approximately 100. Calculation of the infrared intensity of the transitions between the levels requires the derivative of the dipole moment with respect to the puckering coordinate, which we have not calculated. However, the relative intensities of the transitions will be proportional to the expression

$$I(\nu_{f \to i}) \propto \left(\exp\left(-\frac{E_i hc}{kT}\right) - \exp\left(-\frac{E_f hc}{kT}\right) \right) \nu \langle f|Z|i \rangle^2 \quad (8)$$

where $Z = x_1$ or x_2, (or x_1^2, x_2^2, or $x_1 x_2$) and $\langle f|$ and $|i\rangle$ are the final and initial states of the transition with energies E_f and E_i (in cm^{-1}) and the transition frequency ν (in cm^{-1}). Values using this expression are readily calculated with our computer program. Because of the symmetry of this molecule, the puckering motions of the two rings in any given eigenstate occur either in-phase (even) or 180° out-of-phase (odd) and $\langle f|x_1|i \rangle^2 = \langle f|x_2|i \rangle^2$ for all transitions. Also, for transitions between even and odd states $\langle f|x_i|i \rangle^2 \neq 0$ and $\langle f|x_i x_j|i \rangle^2 = 0$, and vice versa for transitions between states of the same symmetry. In the calculation of the transition probabilities, which was done for $T = 300$ K, only transitions originating from the first 50 levels for which the expression eq 8 yielded a value larger than 5×10^{-5} for $Z = x_1$ were considered. The largest values from eq 8 obtained for the transitions were on the order of 0.03. The spectra shown in the figures were generated by multiplying the numbers obtained with eq 8 by 10^5 and representing the transitions on the wavenumber scale with Gaussian profiles of fwhh = 0.5 cm^{-1} and calculating the resulting profile every 0.1 cm^{-1}. The number of transitions obtained with these criteria is on the order of 600 in the spectral range 0−400 cm^{-1}. However, as the computations showed transitions from even the 50th level giving values for eq 8 on the order of 0.006, a fair number of transitions with some intensity are probably missing in the computed spectra in the region around 100 cm^{-1}. This does not affect the conclusions that can be drawn from this study, however. Figure 6 shows the one-dimensional slice along x_2^{min} for the potential energy surface of eq 6 with the lower quantum states and some of the more intense transitions indicated, and Figure 7 shows the same things for the potential energy surface of eq 7. Figures 8 and 9 show the corresponding spectra with the assignment of some of the more prominent bands shown as illustration.

This exercise shows that it probably would be quite difficult to assign the bands in the far-infrared spectrum for this or a related compound without modeling the spectrum. The spectrum
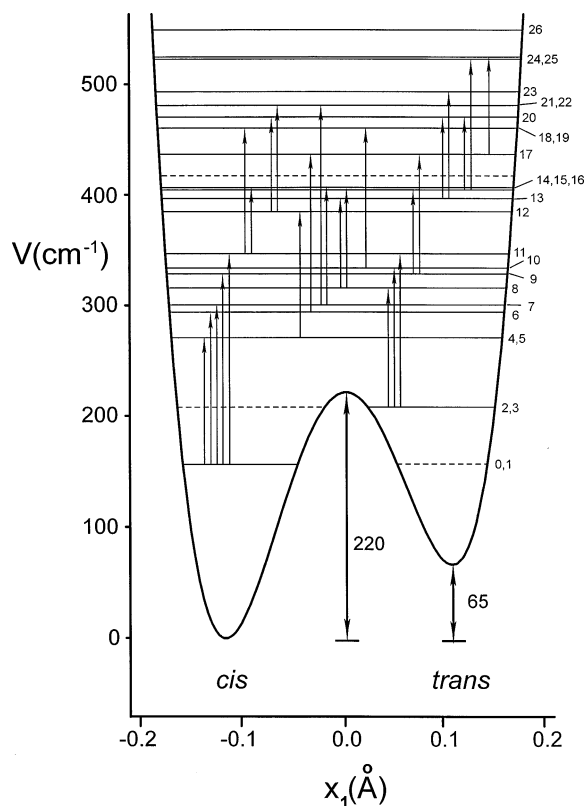
Ring Puckering Vibrations of Bicyclo[3.3.0]oct-1,5-ene

J. Phys. Chem. A, Vol. 108, No. 3, 2004 **413**

Figure 6. One-dimensional slice of the potential energy surface for BCO along the x_2^{min} value (0.115 Å). The dotted line at 408 cm^{-1} indicates the height of the central barrier (nonflapped model).
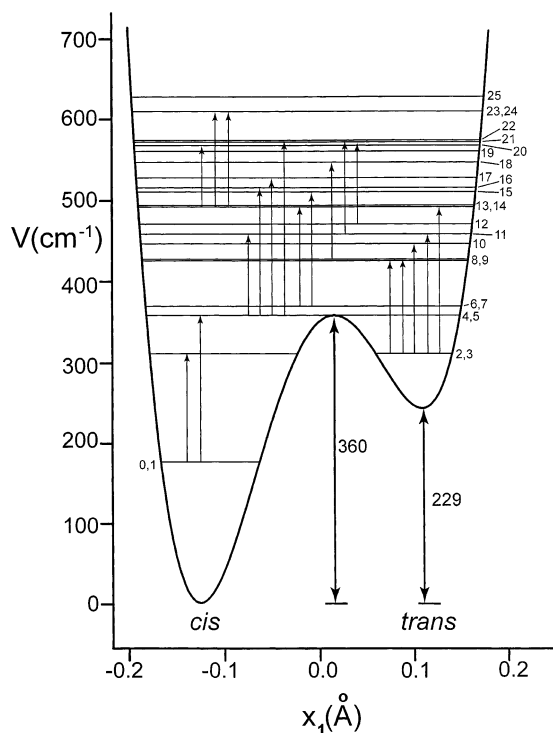

Figure 7. One-dimensional slice of the potential energy surface for BCO along the x_2^{min} value (0.125 Å). The central barrier is at 572 cm^{-1} (flapped model).

is likely to be very rich, showing transitions from many levels with many different transitions from each level occurring with similar probability. Even with a good potential energy model the task would not be simple. In the computed spectra many of the most prominent bands originate from the lower energy states.
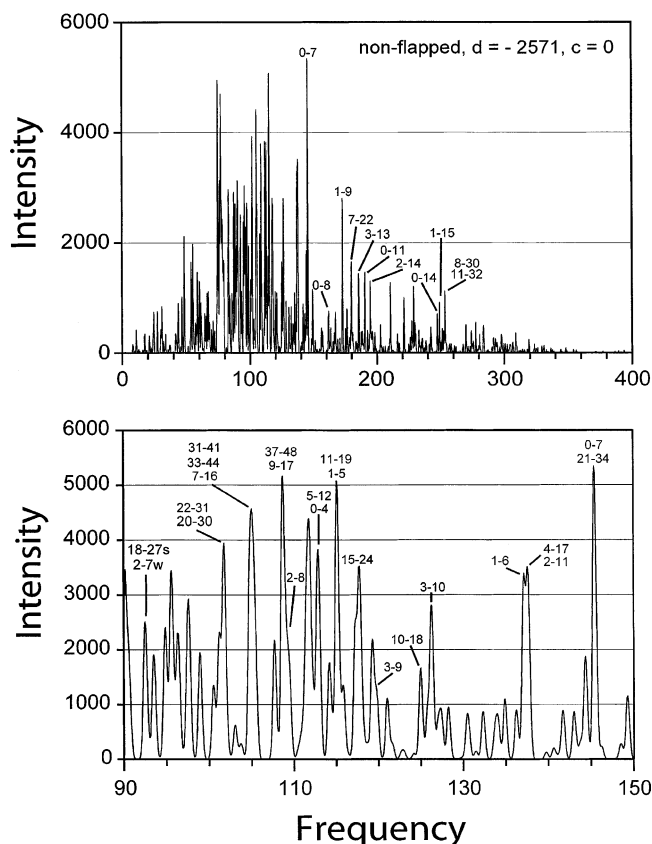

Figure 8. Calculated infrared absorption spectra for the ring-puckering vibrations of BCO (nonflapped model). The assignments of some of the more prominent bands are shown as an illustration.

Derivation of an empiric energy level diagram even for the lowest states from a measured spectrum would nevertheless be difficult because these bands are not well connected by frequency sums or differences, which could be used to confirm the correctness of a proposed diagram. The transitions from the levels in the cis potential well (i.e., 0−4 s, 1−5 s, 0−7 vs, 1−6 s, 0−8 w, 1−9 s, 0−11 m, 1−10 w) do not end with large probability on the same levels as transitions originating from the trans well (i.e., 2−8 m, 3−9 w, 2−11 s, 3−10 s). Most of these bands are not very prominent in the spectrum of the nonflapped molecule among the numerous bands due to transitions between higher levels. This would make the assignments of these bands and the confirmation of a proposed energy diagram with any confidence very difficult. The situation is different in the spectrum obtained with the potential surface of the flapped molecule. There the transitions from the lowest levels are among the most prominent bands, including the transitions 0−3 and 1−2, which are absent in the nonflapped spectrum.

The model used in this study does not describe the spectrum of the puckering motions perfectly. The main shortcoming is that the flapping motion of the two rings has not been taken into account. As shown in a previous study,[7] the kinetic interactions between the flapping and puckering motions can cause a significant redistribution of the puckering levels, which for this molecule might have a significant effect on the ordering of the various transitions present in the spectrum. Taking the flapping motion properly into account would require a three-dimensional calculation, which, considering the large number of quantum states that need to be accurately calculated, would not be feasible at present.

It is nevertheless worthwhile to explore the properties of this model of the puckering motion. Even if a detailed assignment
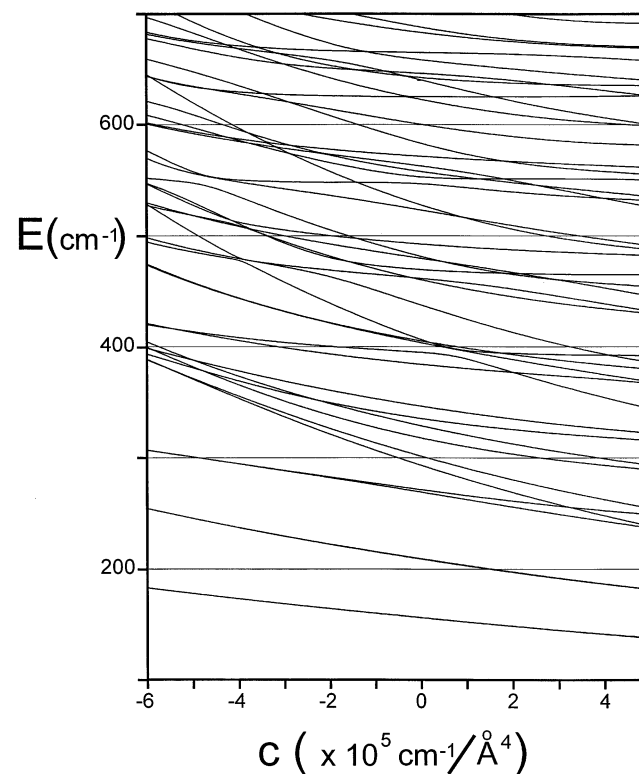
TABLE 4: Effect of Parameters c and d on the Potential Energy Surface for BCO (nonflapped model)

parameter	c: d:	0 0	0 −2571	0 −5000	−5.0 × 10⁵ −2571	5.0 × 10⁵ −2571
$E_{planar} − E_{cis}$		375.4 cm⁻¹	408.8 cm⁻¹	441.6 cm⁻¹	520.7 cm⁻¹	336.5 cm⁻¹
$E_{trans} − E_{cis}$		0 cm⁻¹	65.3 cm⁻¹	127.0 cm⁻¹	83.2 cm⁻¹	53.8 cm⁻¹
$E_{saddle} − E_{cis}$		187.7 cm⁻¹	220.3 cm⁻¹	255.3 cm⁻¹	353.4 cm⁻¹	152.5 cm⁻¹
$x^{min}(cis)$		0.113 Å	0.115 Å	0.117 Å	0.130 Å	0.105 Å
$x^{min}(trans)$		0.113 Å	0.110 Å	0.108 Å	0.124 Å	0.100 Å
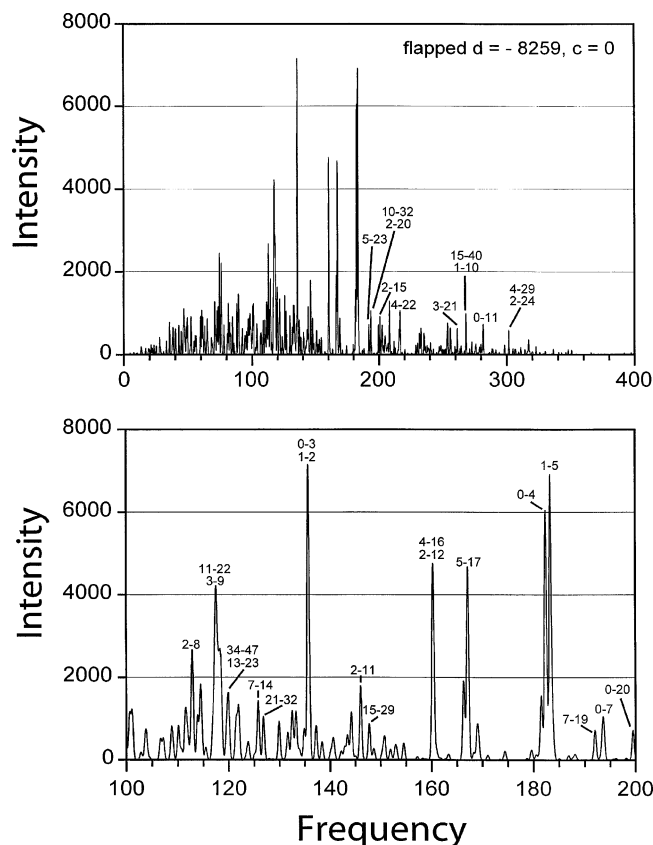
Figure 9. Calculated infrared absorption spectra for the ring-puckering vibrations of BCO (flapped model). The assignments of some of the more prominent bands are shown as an illustration.

of the observed transitions is not accomplished, the overall intensity pattern of the transitions would still be useful for the determination of an empirical potential energy surface. We have calculated the energy levels as functions of the parameter d of eq 2 between 0 and −5000 cm⁻¹/Å² keeping the values of a, b, and c fixed at the values of eq 6, and as functions of the parameter c with a, b, and d fixed at the values of eq 6. The results are shown in Figures 10−12. Table 4 shows how changing c and d modifies the PESs. As can be seen from Table 4, a negative c parameter increases all the barriers and increases the x_1 and x_2 values for the energy minima. The opposite is true for a positive c parameter. The levels 4 and 5 merge (Figure 11) as they drop below the barriers when c decreases. Many higher levels, which approach each other when c decreases, actually cross for $c \sim$ −500 000 cm⁻¹/Å⁴ and thus do not merge in the range of c that was considered.

As is shown in Figure 10, the energies of all levels increase as the value of d gets more negative. The energies are shown on an absolute scale whose zero-point is the energy of the cis minimum energy configuration. Only negative d values are considered, giving the cis configuration the lowest energy, as determined by the ab initio calculations. Positive d values would give the trans configuration the lower energy and would result in slightly different energy level patterns compared to those
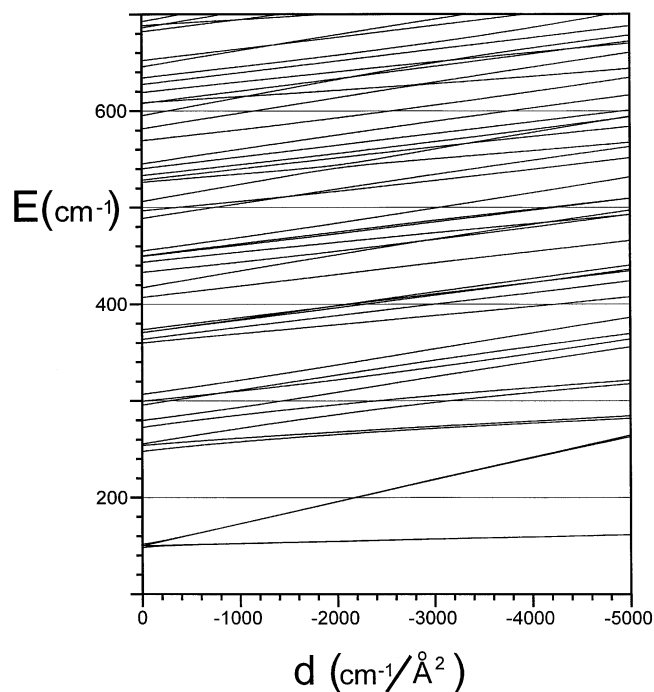
Figure 10. Effect of potential energy parameter d on quantum states (nonflapped model); $c = 0$.

Figure 11. Effect of potential energy parameter c on quantum states (nonflapped model); $d = -2571$ cm⁻¹/Å².

Ring Puckering Vibrations of Bicyclo[3.3.0]oct-1,5-ene

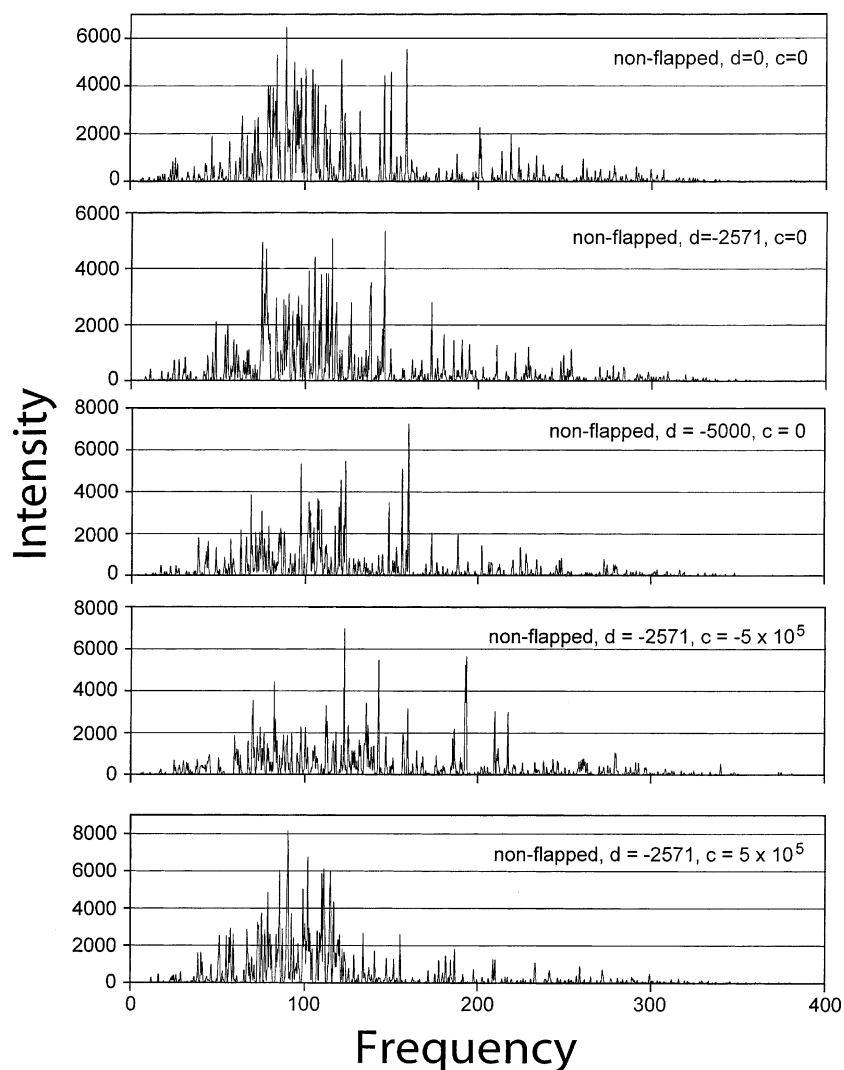*J. Phys. Chem. A, Vol. 108, No. 3, 2004* **415**

Figure 12. Spectra calculated for different values of the parameters c and d of eq 2. The values of parameters a and b are those given in eq 6.

obtained for negative d because of the different kinetic energy contribution to the Hamiltonian. Crossings of energy levels of different symmetry as well as avoided crossings of levels with the same symmetry are observed. Most of the avoided crossings cannot be distinguished from real crossings on the scale at which the figures are made; however, because of the small separation between the two levels at closest approach. For instance, quantum levels 9 and 10 show an avoided crossing for $d \approx 790$ cm^{-1}/Å^2, the distance of closest approach being only 0.004 cm^{-1}. The four lowest energy states would be degenerate in the absence of coupling between the two rings. For $d = 0$ the only coupling is provided by the kinetic energy terms in the Hamiltonian, resulting in a splitting of ≈ 3.6 cm^{-1} between the lowest and highest of these four levels. The splitting between the levels in the cis and trans wells is largest (≈ 1.7 cm^{-1}) for $d = 0$ and decreases to a few tenths of a wavenumber as the energy difference of the cis and trans conformers increases. With decreasing d the energies of levels 2 and 3 increase as the energy of the minimum of the trans conformation of the molecule increases. The levels 1 and 2 actually cross at $d = \approx -6.7$ cm^{-1}/Å^2 and levels 2 and 3 at $d \approx -925$ cm^{-1}/Å^2. The height above the cis conformation energy minimum of the energy of levels 0 and 1, which correspond to the in-phase and out-of-phase puckering of the to rings in the cis conformation, is fairly unaffected by the parameter d. In Figure 12 a few representative spectral intensity distributions are shown for different values

of the d parameter. Figure 11 shows the energy levels as functions of the c parameter with $d = 2571$ cm^{-1}/Å^2 and a few of the corresponding spectra are also shown in Figure 12. It is evident from these results that the quantum states for the puckering of BCO are quite sensitive to both the degree of interaction between the two rings and the energy difference between the cis and trans forms and the barrier to the cis–trans interconversion.

Figures 10 and 11 clearly show that it would be quite difficult to optimize the parameters of the potential energy surface using the method described in ref 11, even if an empirical energy level structure based on the observed spectrum could be constructed. At every crossing of energy levels involved in the assigned transitions used in the optimization, the dependence of the calculated frequencies on the PES parameters would change, ruining the optimization process. For each iteration of the optimization, the assignments of the computed levels would therefore have to be checked by inspection of the computed intensities and corresponding changes made to the input, if necessary.

Conclusions

Both experimental data and ab initio calculations indicate that BCO can exist in both cis and trans conformations, with the former being lower in energy. This results in a potential energy

416 *J. Phys. Chem. A, Vol. 108, No. 3, 2004*

Autrey et al.

surface for the two ring-puckering vibrations, which has two pairs of minima at different energies. This PES gives rise to a complicated pattern of energy states, between which the low-frequency vibrational transitions can occur.

In this work we have generated two plausible potential energy surfaces based on ab initio calculations in order to better understand the pattern of quantum states and the vibrational spectra arising from them. We have also investigated the effect of the potential energy terms reflecting ring-to-ring interaction and the magnitude of the cis−trans energy difference. Although the results cannot be compared to experimental data at present, they should provide a framework for future studies on bicyclical molecules of this type.

References and Notes

(1) Autrey, D.; Haller, K.; Laane, J.; Mlynek, L.; Hoopf, H. *J. Phys. Chem. A.* **2004**, *108*, 403.

(2) Laane, J. *J. Phys. Chem. A.* **2000**, *33*, 7715.

(3) Laane, J. *Int. Rev. Phys. Chem.* **1999**, *18*, 301.

(4) Laane, J. *Annu. Rev. Phys. Chem.* **1994**, *45*, 179.

(5) Laane, J. In *Structures and Conformations of Non-Rigid Molecules*; Laane, J., Dakkouri, M., van der Veken, B., Oberhammer, H., Eds.; Amersterdam, 1993; Chapter 4.

(6) Klots, T.; Sakurai, S.; Laane, J. *J. Chem. Phys.* **1998**, *108*, 3531.

(7) Sakurai, S.; Meinander, N.; Laane, J. *J. Chem. Phys.* **1998**, *108*, 3537.

(8) Bondoc, E.; Sakurai, S.; Morris, K.; Chiang, W.-Y.; Laane, J. *J. Chem. Phys.* **1999**, *103*, 8772.

(9) Sakurai, S.; Meinander, N.; Morris, K.; Laane, J. *J. Am. Chem. Soc.* **1999**, *121*, 5056.

(10) Laane, J.; Bondoc, E.; Sakurai, S.; Morris, K.; Meinander, N.; Choo, J. *J. Am. Chem. Soc.* **2000**, *122*, 2628.

(11) Meinander, N.; Laane, J. *J. Mol. Struct.* **2001**, *569*, 1.

(12) Laane, J.; Harthcock, M. A.; Killough, P. M.; Bauman, L. E.; Cooke, J. M. *J. Mol. Spectrosc.* **1982**, *91*, 286.

(13) Harthcock, M. A.; Laane, J. *J. Mol. Spectrosc.* **1982**, *91*, 300.

(14) Schmude, R. W.; Harthcock, M. A.; Kelly, M. B.; Laane, J. *J. Mol. Spectrosc.* **1987**, *124*, 369.

(15) Tecklenburg, M. M.; Laane, J. *J. Mol. Spectrosc.* **1989**, *137*, 65.

(16) Strube, M. M.; Laane, J. *J. Mol. Spectrosc.* **1988**, *129*, 126.

(17) Laane, J.; Lord, R. C. *J. Chem. Phys.* **1967**, *47*, 4941.

(18) Bauman, L. E.; Killough, P. M.; Cooke, J. M.; Villarreal, J. R.; Laane, J. *J. Phys. Chem.* **1982**, *86*, 2000.